Original Article

Pulmonary Circulation

Orotracheal treprostinil administration attenuates bleomycin-induced lung injury, vascular remodeling, and fibrosis in mice

Ioanna Nikitopoulou[1,*], Nikolaos Manitsopoulos[1,*], Anastasia Kotanidou[1,2], Xia Tian[3], Aleksandar Petrovic[3], Christina Magkou[4], Ioanna Ninou[5], Vassilis Aidinis[5], Ralph T. Schermuly[3], Djuro Kosanovic[3,6] and Stylianos E. Orfanos[1,2,7]

[1]GP Livanos and M Simou Laboratories,1st Department of Critical Care & Pulmonary Services, Medical School, National & Kapodistrian University of Athens, Evangelismos Hospital, Athens, Greece; [2]1st Department of Critical Care & Pulmonary Services, Medical School, National & Kapodistrian University of Athens, Evangelismos Hospital, Athens, Greece; [3]Universities of Giessen and Marburg Lung Center, Member of the German Center for Lung Research (DZL), Justus-Liebig University, Giessen, Germany; [4]Department of Pathology, Evangelismos Hospital, Athens, Greece; [5]Institute of Immunology, Biomedical Sciences Research Center Alexander Fleming, Athens, Greece; [6]Sechenov First Moscow State Medical University (Sechenov University), Moscow, Russia; [7]2nd Department of Critical Care, Medical School, National & Kapodistrian University of Athens, "Attikon" Hospital, Haidari, Athens, Greece

Abstract

Pulmonary fibrosis is a progressive disease characterized by disruption of lung architecture and deregulation of the pulmonary function. Prostacyclin, a metabolite of arachidonic acid, is a potential disease mediator since it exerts anti-inflammatory and anti-fibrotic actions. We investigated the effect of treprostinil, a prostacyclin analogue, in bleomycin-induced experimental pulmonary fibrosis. Bleomycin sulfate or saline was administrated intratracheally to mice ($n = 9–10$/group) at day 0. Orotracheal aspiration of treprostinil or vehicle was administered daily and started 24 h prior to bleomycin challenge. Evaluation of lung pathology was performed in tissue samples and bronchoalveolar lavage fluid collected 7, 14 and 21 days after bleomycin exposure. Lung injury was achieved due to bleomycin exposure at all time points as indicated by impaired lung mechanics, pathologic lung architecture (from day 14), and cellular and protein accumulation in the alveolar space accompanied by a minor decrease in lung tissue VE-cadherin at day 14. Treprostinil preserved lung mechanics, and reduced lung inflammation, fibrosis, and vascular remodeling (day 21); reduced cellularity and protein content of bronchoalveolar lavage fluid were additionally observed with no significant effect on VE-cadherin expression. Bleomycin-induced collagen deposition was attenuated by treprostinil from day 14, while treprostinil involvement in regulating inflammatory processes appears mediated by NF-κB signaling. Overall, prophylactic administration of treprostinil, a stable prostacyclin analogue, maintained lung function, and prevented bleomycin-induced lung injury, and fibrosis, as well as vascular remodeling, a hallmark of pulmonary hypertension. This suggests potential therapeutic efficacy of treprostinil in pulmonary fibrosis and possibly in pulmonary hypertension related to chronic lung diseases.

Keyword

inflammation, fibrosis, bleomycin, prostacyclin, pulmonary hypertension, treprostinil

Date received: 24 April 2019; accepted: 4 September 2019

Pulmonary Circulation 2019; 9(4) 1–14
DOI: 10.1177/2045894019881954

Introduction

Idiopathic pulmonary fibrosis (IPF) is a chronic, fatal lung disease of unknown etiology with a median survival of patients not exceeding three to five years from diagnosis.[1,2] The result of progressive lung structure disruption is functional impairment and subsequently excessive morbidity and mortality. Global incidence slowly increases and usually

*These authors contributed equally to this work.

Corresponding author:
Stylianos E. Orfanos, 2nd Department of Critical Care, Attikon University Hospital, 1, Rimini St., Haidari, Athens 12462, Greece.
Email: stylianosorfanosuoa@gmail.com

60–70 year old males are affected.[3] Pulmonary hypertension (PH) is a frequent complication of IPF and other chronic lung diseases,[4] increasing the morbidity and mortality of such patients. Several multicenter clinical trials have been conducted for IPF, but only two drugs (pirfenidone and nintedanib) were proved to be effective as disease-modifying therapies.[5] However, for a number of patients the only effective treatment will still be lung transplantation.[1]

IPF pathophysiology involves alveolar epithelial cell damage usually of repetitive nature, accompanied by deregulated wound healing. This leads to excessive extracellular matrix (ECM) deposition and eventually fibrosis. The animal model most widely used to resemble the human disease is the bleomycin (BLM) mouse model.[6]

Previous studies have revealed possible target molecules participating in IPF pathogenesis. Eicosanoids are signaling molecules produced from arachidonic acid through cyclooxygenase (COX) pathways, and their group includes among others prostaglandins (PGI_2, PGF_{2a}, PGD_2, and PGE_2), leukotrienes and thromboxanes (TX). Notably, prostaglandins have been previously linked to lung fibrotic processes. Prostacyclin (PGI_2) elevates the levels of cyclic adenosine monophosphate (cAMP) and may thus control inflammation and fibrosis.[7] In human fibroblasts from IPF patients, the ratio of PGI_2 to profibrotic thromboxane A_2 (TXA_2) was found lower compared to healthy lung fibroblasts, suggesting a trend towards fibrogenesis.[8] Besides, studies on human fetal lung fibroblasts revealed that two PGI_2 analogues were able to inhibit fibroblast migration,[9] and most importantly prostacyclin analogues protected COX-$2^{-/-}$ mice from BLM-induced pulmonary fibrosis.[10] Prostaglandin E_2 (PGE_2) and TXA_2 are both involved in lung fibrosis; inhibition of TXA_2 synthesis was able to attenuate BLM-induced fibrosis in mice[11] and PGE_2 was shown to inhibit fibroblast proliferation[12] and collagen production.[13]

Treprostinil is a prostacyclin analogue previously shown to inhibit the recruitment of circulating fibrocytes in PH.[14] Thus, the aim of the study was to delineate whether treprostinil controls inflammation and pulmonary fibrosis, while its effect on vascular remodeling was additionally studied. Experimental approach involved intratracheal exposure of mice to BLM and daily treatment with the stable prostacyclin analogue treprostinil through the inhaled route. Some of the results presented here were previously reported in the form of an abstract.[15]

Methods

Animals

This study was approved by the Evangelismos Hospital Research Review Board – Ethics Committee and by the Veterinary Service of the governmental prefecture of Attica, Greece (approval protocol number 788/11 February 2014). All experiments were performed in compliance with the European Union Directive 2010/63/EU and with the ARRIVE guidelines. Handling was performed under deep anesthesia induced by intraperitoneal injection of ketamine/xylazine (100 mg/kg and 10 mg/kg, respectively). Animal distress and suffering were minimized, and exsanguination was used as the method of euthanasia. Mice were bred and maintained on the C57BL/6 background in the animal facilities of the ''BSRC Alexander Fleming'' (Athens, Greece) under specific pathogen–free conditions. All experiments were performed at the Animal Model Research Unit of Evangelismos Hospital where animals are kept at 20–22°C, 55 ± 5% humidity, and 12-h light-dark cycle. Food and water were provided *ad libitum*.

BLM model

BLM sulfate (2 U/kg) was administered intratracheally to wild type (WT) mice via tracheotomy under intraperitoneal ketamine/xylazine anesthesia. Mice in the control group received saline (SAL) alone.

Experimental design

Mice were randomly assigned into experimental groups and were monitored twice daily. The time points studied are 7, 14 and 21 days post BLM or SAL. Orotracheal aspiration of treprostinil (TREP, TYVASO® United Therapeutics, Maryland, USA; 0.6 mg/ml) or vehicle (VEH; NaCl, $Na_3C_6H_5O_7$, NaOH, and HCl in sterile water, at concentrations same as in Tyvaso solution) was performed twice daily (12-h intervals) starting 24 h (day −1) prior to BLM or SAL exposure (day 0) and lasting for the whole duration of the experiment. All time points include four experimental groups ($n = 9$–10 animals per group): (1) SAL/VEH group receiving orotracheally vehicle solution starting at day −1, and SAL at day 0; (2) SAL/TREP group receiving treprostinil (total amount of 80 μg/kg/day in two doses; i.e. 40 μg/kg BID, based on previous studies[16]) starting at day −1, and SAL at day 0; (3) BLM/VEH group treated orotracheally with vehicle starting at day −1, and BLM at day 0; (4) BLM/TREP group receiving orotracheally treprostinil, as per group 2, starting at day −1, and BLM at day 0.

Samples

Mice were sacrificed under deep anesthesia by exsanguination. A heparinized 27 g syringe was used to obtain arterial blood samples from the abdominal large vessels. Serum was extracted from blood samples via centrifugation at 1500 r/min for 10 min at 4°C and stored at −80°C. Bronchoalveolar lavage fluid (BALF) was collected as previously described,[17] cellular components were removed via centrifugation at 1500 r/min for 10 min at 4°C and the

supernatants were kept at −80°C. Lungs were collected and stored at −80°C or kept in 4% paraformaldehyde.

Lung mechanics

Lung mechanics assessment was performed at all-time points; 7, 14, and 21 days after BLM or SAL exposure (day 0), each animal was cannulated following deep anesthesia and was shortly ventilated for lung mechanics evaluation purposes. Tissue elastance and static compliance (Cst) were measured by means of a small animal ventilator (FlexiVent, Scireq, Ontario, Canada), using the low frequency forced oscillation technique and static pressure-volume curve of respiratory system. The ventilation protocol consists of 8 ml/kg tidal volume (Vt) and 150 breaths per minute while positive end expiratory pressure (PEEP) was adjusted at 2 cm/H_2O. Standardization of respiratory function required the performance of two total lung capacity maneuvers (deep inflations) following the short run-in period. Data collection of lung mechanics started after 1 min of Vt ventilation. Respiratory function evaluation was achieved via the assessment of tissue elastance coefficient (H) and Cst. The former was collected via the forced oscillation technique and was estimated by the use of the Constant Phase model. A 30-s interval was separating each measurement. The Cst of the respiratory system was then evaluated using data by three quasi-static PV curves, and more specifically by fitting of the Salazar–Knowles equation to the expiratory part of the loop.[18]

BALF total protein and differential cell count

Total protein concentration in BALF was determined using the Bio-Rad Dc Protein Assay kit (Bio-Rad Laboratories, Hercules, CA, USA). A Neubauer hemocytometer was used for the determination of total cell counts. Following total cell number quantification in BALF, cellular components were removed via centrifugation at 1500 r/min for 10 min and resuspended in PBS; $50–70 \times 10^3$ cells per glass slide were centrifuged (Cytospin3, SHANDON), air dried at room temperature and stained with May-Grunwald–Giemsa. Optical observation was used for differential cell count via an optical microscope (Olympus BX50).

Histopathology

Sections (5 μm) of paraffin-embedded tissues were stained with hematoxylin and eosin (H&E) according to standard histological procedures and optical observation of the microscopic lung structure was performed blindly by an expert pathologist. Lung inflammation scoring was performed according to Murao et al.[19] Focal thickening of alveolar membranes, congestion, and interstitial and intra-alveolar neutrophil infiltration were assigned a score from 0 to 3 based on the absence (0) or presence to a mild (1), moderate (2), severe (3) degree and a total cumulative histology score was determined.

Immunostaining and pulmonary vascular morphometry

From paraffin-embedded lungs, 4 μm sections were obtained and staining was performed with an anti-alpha-SMA antibody (Abcam plc, UK). After incubation with an HRP-conjugated secondary antibody, 3, 3′ diaminobenzidine was used as chromogen and sections were counterstained with hematoxylin. Morphometry was performed as previously described.[20] Small vessels from 20 to 70 μm in diameter were counted and characterized blindly as fully muscularized (>75% α-SMA staining), partially muscularized (up to 75%) or non-muscularized.

Soluble collagen evaluation

Lung soluble collagen content was evaluated with Sircol collagen assay kit; 50 mg of each tissue was homogenized and incubated in a pepsin solution at 4°C for 24 hours, and the concentration of soluble collagen in the supernatant was assessed according to the manufacturer's protocol.

Masson trichrome stain

Lung sections were stained with a Sigma Aldrich stain kit following the manufacturer's protocol. Optical observation of the samples was performed blindly by a specialist. Aschroft test was used for the quantification of fibrotic injury in the lung according to Hubner et al.[21]

Enzyme-linked immunosorbent assay

Quantification of osteopontin and periostin was performed in BALF samples from all mice using commercial Elisa kits (R&D Systems, Inc., MN, USA) according to the manufacturer's protocol. Samples from all time points were prepared in duplicate.

Western blotting

SDS-PAGE was performed on 10% polyacrylamide gels and samples from all groups of time point day 21 were transferred to Immobilon-P PVDF membranes (Millipore, 0.45 μl pore size, Millipore Corporation, Billerica, MA, USA). Membranes were probed with one of the following primary antibodies: phospho-JNK, JNK, phospho-p44/42 MAPK, p44/42 MAPK, phospho-p38, p38, phospho-IκBα (Cell Signaling, Danvers, MA, USA), VE-cadherin (Santa Cruz Biotechnology, Texas, USA) and actin (Millipore, Temecula, CA, USA). Protein bands were detected by chemiluminescence (Santa Cruz Biotechnology, Texas, USA). For quantification, densitometric analysis was performed.

Statistical analysis

Data are presented as means ± SEM. Comparisons among groups were made using one-way randomized ANOVA, followed by Newman–Keuls or Tukey's multiple comparisons tests, as appropriate. Differences were considered significant when $p < 0.05$ ($^{*}p < 0.05$, $^{**}p < 0.01$, $^{***}p < 0.001$).

Results

Treprostinil treatment preserves lung mechanics and maintains lung function of BLM-challenged mice

Lung injury due to BLM affects respiratory function. Impaired breathing in our model is denoted by a decrease in lung Cst and an increase in elastance (H). In detail, Cst decreases at all time points were observed (Fig. 1a–c) in animals of the BLM/VEH group, with concurrent H increases (Fig. 1d–f) peaking at day 21 (67.7 ± 8.9 vs. $34.95 \pm 4.3\,cmH_2O/ml$). To test our orotracheal method, Evans Blue was given to mice in preliminary experiments, and homogeneous lung distribution was confirmed (data not shown). Daily treatment with treprostinil, starting at day −1, attenuated BLM-induced lung mechanical dysfunction, as the BLM/TREP group showed a smaller decrease of Cst at all three time points, reaching a statistical significance at day 21 (Fig. 1c, 0.0424 ± 0.006 vs. $0.070 \pm 0.006\,ml/cmH_2O$). Remarkably, in the BLM/TREP group, H decreased in a statistically significant way at all time points (Fig. 1d–f).

Treprostinil maintains lung architecture and prevents BLM-induced lung injury

Lung injury due to BLM is characterized by alveolar wall thickening and cell accumulation. Eventually normal lung structure is replaced by "scar" tissue formation due to excessive collagen deposition. In our experimental protocol, histological evaluation revealed a mild lung injury of the BLM/VEH group starting (non-significantly) at day 7 and progressing until day 21 (Fig. 2). Treprostinil administration attenuated BLM-induced lung injury at days 14 and 21; histopathological score was significantly lower in BLM/TREP group compared to BLM/VEH (Fig. 2b and c) and representative tissue histology showed less extensive inflammation and focal alveolar thickening in the BLM/TREP group (Fig. 2d–f).

Treprostinil effect on BLM-induced BALF cell infiltration and increased vascular permeability

BLM-induced inflammatory response is characterized by an increase of the cellular content in the alveolar compartment. Accumulation of white blood cells occurs, as well as disruption of the endothelial barrier and increased protein content in BALF. BLM-challenged mice in our experiment showed excessive alveolar flooding (Fig. 3). In particular, a marked increase in BALF total cellularity was observed at all time points (Fig. 3a–c) and a peak was reached at day 21 (total

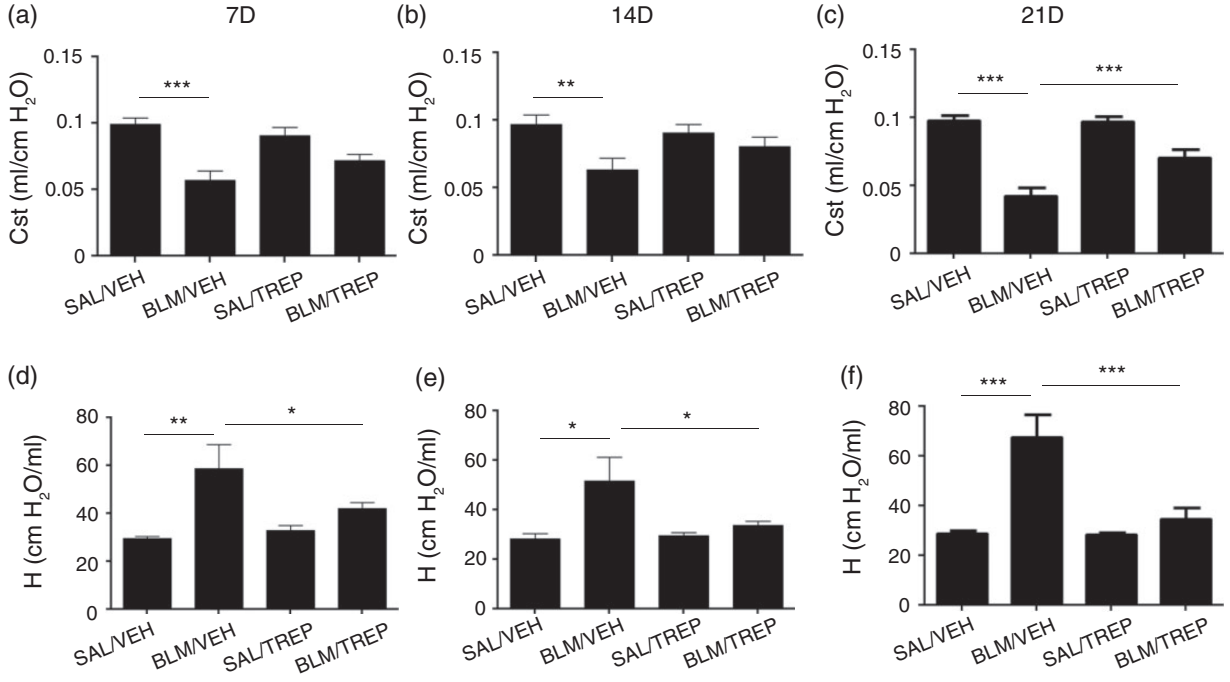

Fig. 1. Effect of orotracheal treprostinil (TREP) administration on lung mechanics of all animal groups 7, 14 and 21 days after intratracheal injection of bleomycin (BLM) or saline (SAL). BLM reduced lung static compliance (a–c) and increased tissue elastance (d–f), phenomena that were reversed in the BLM/TREP treated group. Results are expressed as mean ± SEM, $n = 9$–10 mice per group. One-way ANOVA followed by Newman–Keuls post hoc test was used for the comparison among groups. Cst: static compliance; H: tissue elastance coefficient; 7D: 7 days; 14D: 14 days; 21D: 21 days.

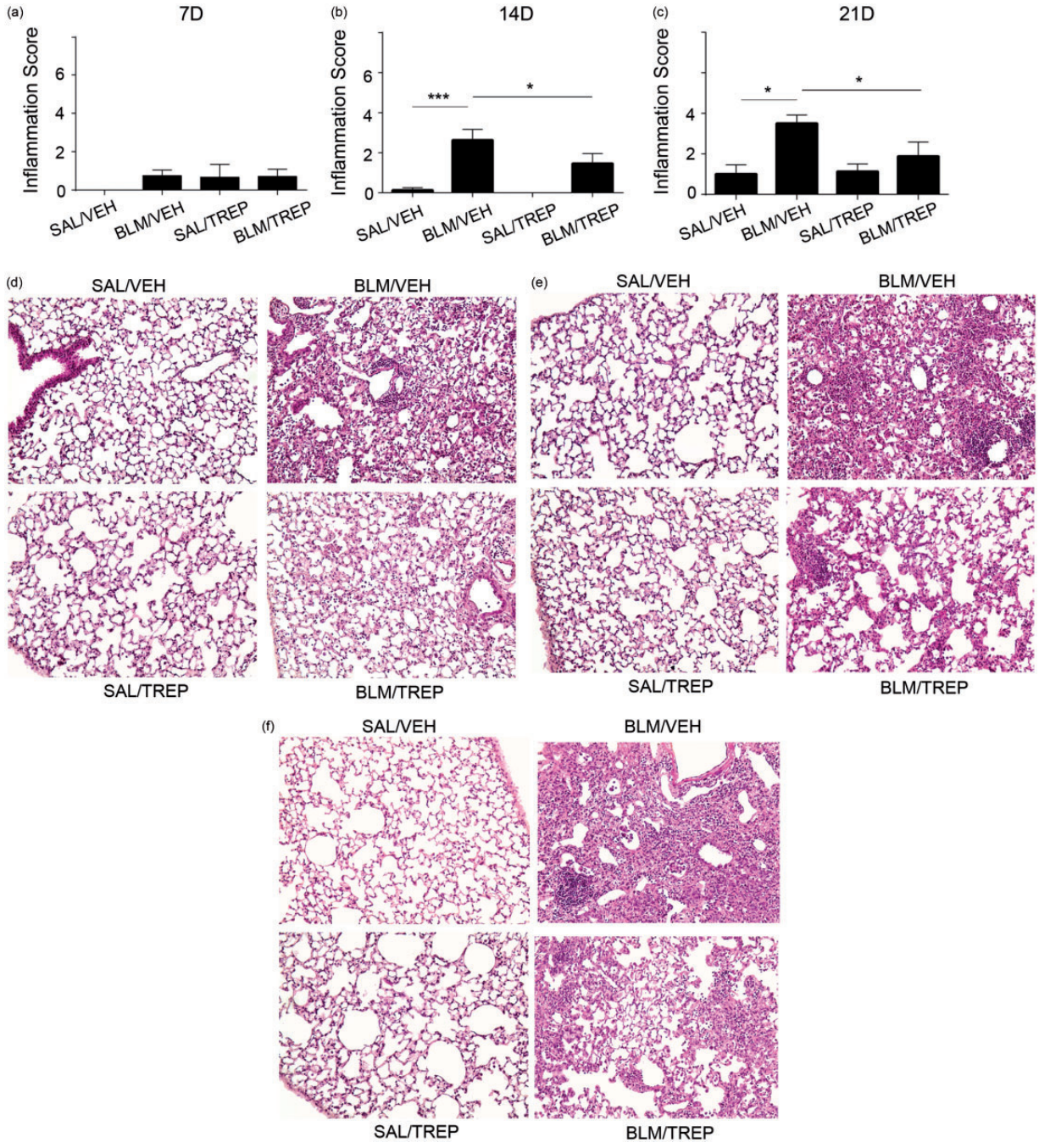

Fig. 2. Orotracheal treprostinil (TREP) administration attenuates bleomycin (BLM)-induced pulmonary inflammation and fibrosis. Following histological analysis of murine lungs included in each group at every time point, lung injury was quantified (a–c). Results are expressed as mean ± SEM, $n = 9$–10 mice per group. One-way ANOVA followed by Newman–Keuls post hoc test was used for comparison among groups. Representative H&E stainings are shown in (d–f); mice treated with bleomycin and treprostinil show less leukocyte accumulation, alveolar structure distortion and collagen deposition (d: 7D, e: 14D, f: 21D). SAL: saline; VEH: vehicle; 7D: 7 days; 14D: 14 days; 21D: 21 days.

score 985.9 ± 158.1 cells/ml). Additionally, examination of cell population in BALF revealed a neutrophil increase (Fig. 3d–f), with accumulation reaching a peak at day 21 (neutrophils % of total cells: 35.64 ± 6.7). Exposure to BLM led to BALF protein enrichment in BLM/VEH group starting at day 7 (Fig. 3g) and increasing at days 14 and 21 (Fig. 3h and i). Treprostinil managed to attenuate the aforementioned phenomena; pleocytosis in BALF was significantly reduced in BLM/TREP group 7, 14 and 21 days after BLM (Fig. 3a–c). Neutrophil levels in BALF also showed a decrease upon treprostinil treatment at all time points; notably, 14 and 21 days after BLM neutrophil counts of BLM/TREP mice reached those of the control groups (SAL/VEH, SAL/TREP) (Fig. 3e and f). Protein

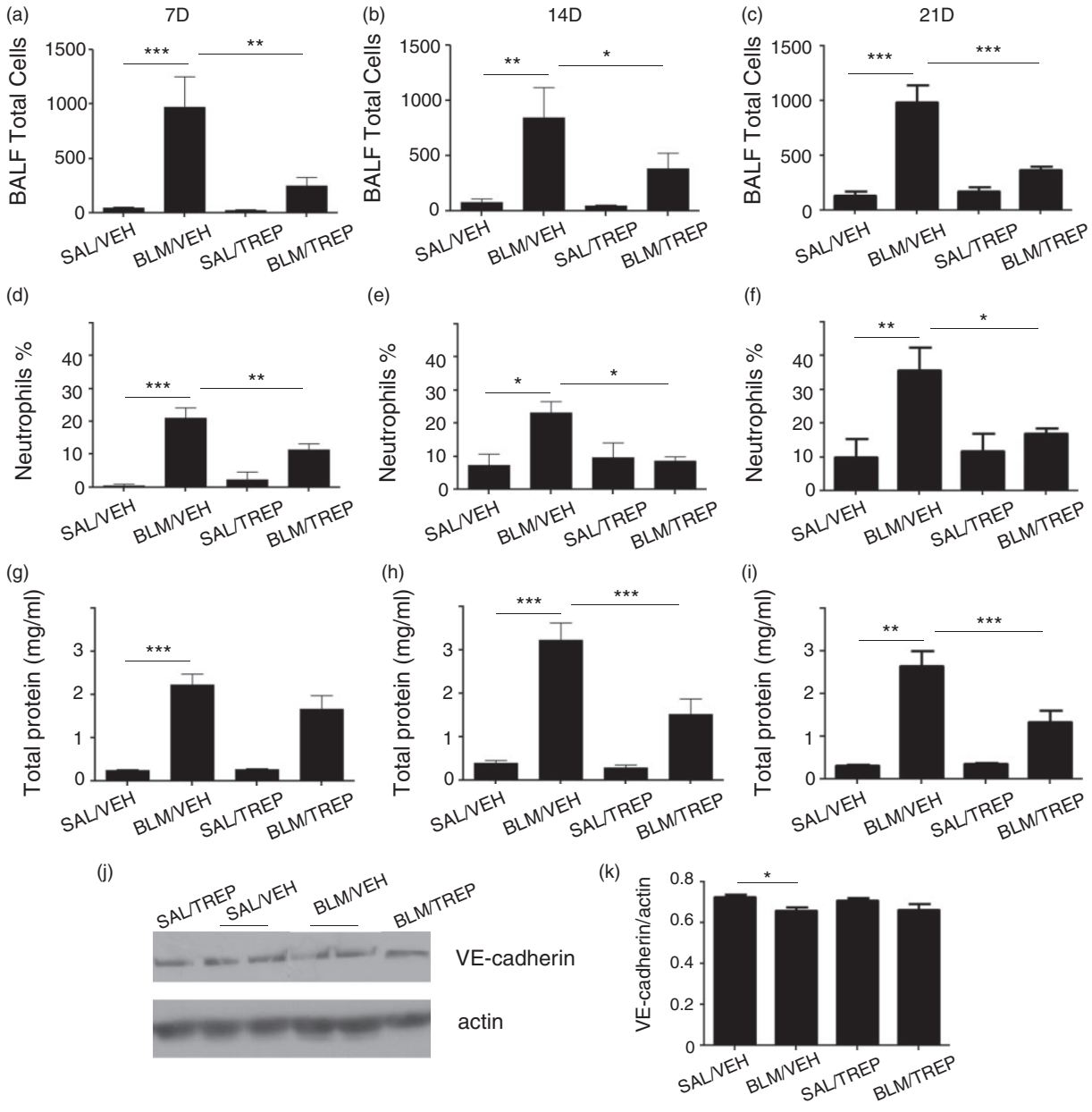

Fig. 3. Effect of treprostinil (TREP) treatment on inflammatory cell infiltration in bronchoalveolar lavage fluid (BALF) and on endothelial barrier disruption. Total cell counts (a–c) and neutrophil counts (d–f) in BALF collected at days 7, 14 and 21 post bleomycin (BLM). Collection of inflammatory cells in airways was significantly reduced in mice receiving BLM and treprostinil, compared to those receiving only BLM. Protein leakage in the airspace induced by BLM was reduced significantly at later stages, as shown by total protein concentrations (g–i). (j, k): Representative Western blot for VE-cadherin in mouse lung tissues 14 days post bleomycin and respective protein quantification after normalization with actin. Results are expressed as mean ± SEM, $n = 9$–10 mice per group. One-way ANOVA followed by Newman–Keuls post hoc test was used for comparison among groups. 7D: 7 days; 14D: 14 days; 21D: 21 days.

content in BALF showed a decrease upon treprostinil treatment and statistically significant differences were observed at time points of 14 and 21 days (Fig. 3h and i). In order to examine the vascular endothelial integrity of our model, apart from total protein levels in BALF, levels of vascular endothelial (VE)-cadherin in lung tissues were also determined. VE-cadherin is a protein of the adherens junctions, essential for the maintenance of the endothelial barrier. In our model, we observed a small but significant decrease 14 days after BLM challenge not affected by treprostinil (Fig. 3j and k); however, this decrease was not maintained at the time point of 21 days (data not shown).

Treprostinil effect on BLM-induced increase in pulmonary vascular muscularization

In order to determine whether pulmonary vascular remodeling is affected by treprostinil, the degree of pulmonary vessel

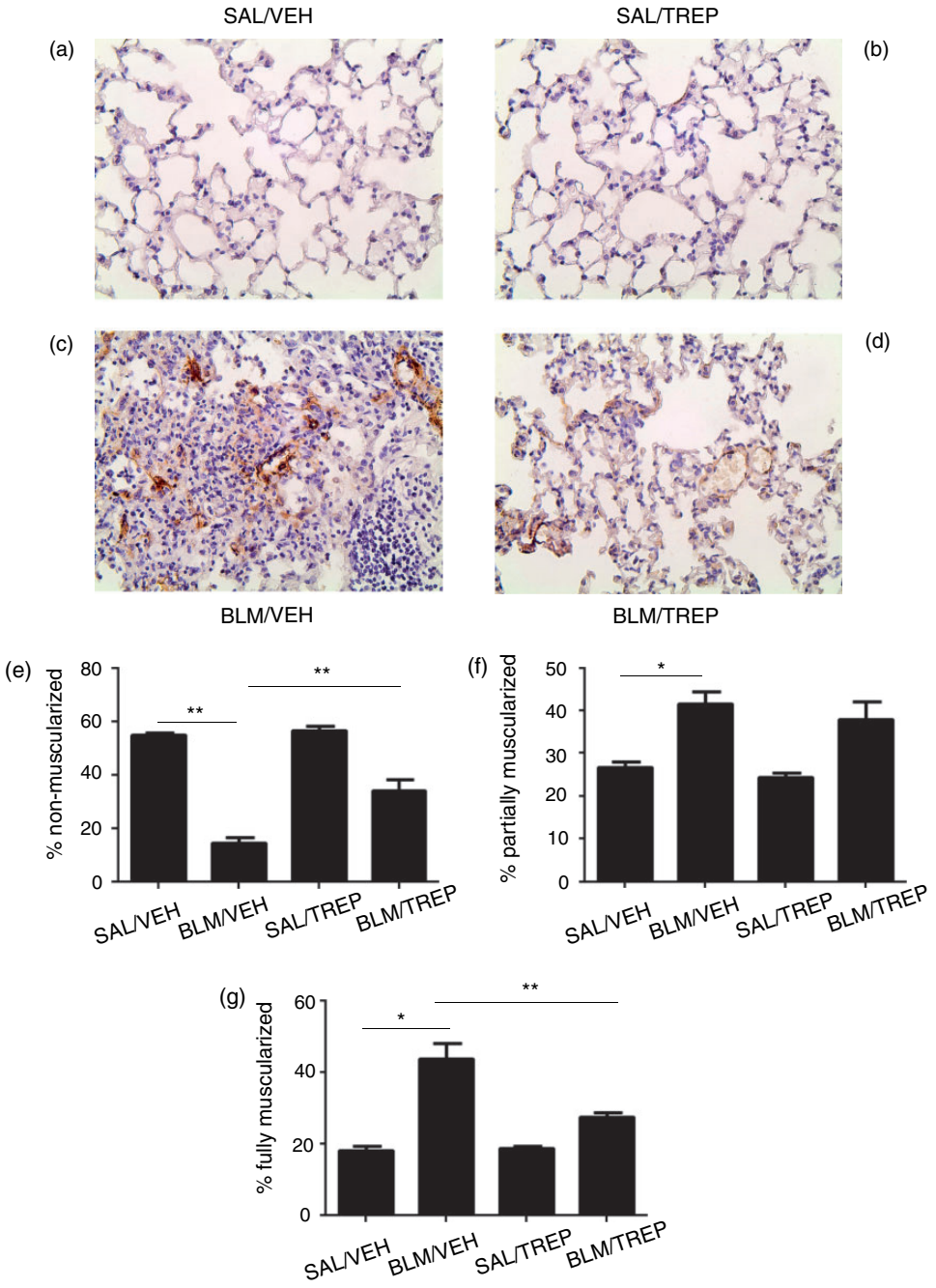

Fig. 4. Effect of treprostinil (TREP) treatment on pulmonary vascular remodeling in bleomycin (BLM)-challenged mice. Lung sections were stained for alpha (α)-smooth muscle actin, and pulmonary vascular remodeling was analyzed, in vessels of 20–70 μm diameter, 21 days post BLM. Representative images from all groups are shown (a–d): (a): animal treated with SAL and VEH, (b): animal treated with SAL and TREP, (c): animal treated with BLM and VEH, (d): animal treated with BLM and TREP. (e–g): Percentages of non-, partially and fully muscularized vessels are shown for each group. Data are presented as mean ± SEM ($n = 4$–7 mice per group). One-way ANOVA followed by Tukey's multiple comparisons test was used for comparison among groups. SAL: saline; VEH: vehicle.

muscularization at Day 21 was assessed (Fig. 4). In agreement with previous studies,[22] BLM caused the development of pulmonary vascular remodeling, as evident from the significant reduction in % of non-muscularized vessels and augmentation in % of muscularized vessels, in comparison to the control group (Fig. 4e–g). TREP treatment in BLM-challenged mice significantly ameliorated this process, as demonstrated by increase in % of non-muscularized vessels and decrease in % of fully muscularized vessels.

Treprostinil administration attenuates collagen deposition

Fibrotic phenotype due to BLM is established seven days from the time of exposure. In our experimental setting,

BLM-induced cell accumulation and alveolar thickening eventually resulted in excessive collagen production and ECM deposition that altered normal lung structure, creating a scar formation (Fig. 5g–i). Soluble collagen levels in BLM/VEH group showed a slight increase at day 7, and as disease progressed they reached a peak at day 21 (Fig. 5c). Histological evaluation of lung sections, specifically for collagen, revealed sporadic collagen deposition at day 7 (Fig. 5g), fibrotic lesion presence at day 14 (Fig. 5h), and excessive fibrotic lung areas at day 21 (Fig. 5i). Fibrotic scores were given accordingly by a specialist using the Ashcroft methodology. Significant formation of fibrosis started at day 7 for the BLM/VEH group, while at day 21, an almost 3-fold increase of the fibrotic areas of the BLM/VEH group was observed compared to the SAL/VEH group (Fig. 5f). Treprostinil treatment resulted in soluble collagen levels decrease at days 14 and 21 (Fig.5b and c) compared to the BLM/VEH group levels (677.8 ± 31.03 vs 861.7 ± 44.87 μg/ml; day 21). Histological evaluation further revealed that in the BLM group receiving treprostinil, fibrosis formation was attenuated, and corresponding fibrotic scores of BLM/TREP and BLM/VEH groups showed significant differences at days 14 and 21 (Fig. 5e and f).

Treprostinil administration affects the levels of IPF candidate biomarkers

Osteopontin and periostin are proteins reported to be instrumental in IPF and experimental pulmonary fibrosis. We observed increased levels of osteopontin in the BALF of the BLM-challenged mice, beginning from day 7 and remaining elevated until day 21 (Fig. 6a–c). The peak of osteopontin levels was observed in BALF of BLM/VEH group at day 21 post BLM (470.2 ± 42.23 μg/ml) (Fig. 6c). Treprostinil administration significantly lowered osteopontin levels at day 14, continuing until day 21 (325 ± 73.13 μg/ml). Levels of the matricellular protein periostin were measured in BALF, and BLM was shown to drastically increase periostin from day 7 until day 21 (Fig. 6d–f). Upon treprostinil treatment, periostin levels gradually dropped, with significant differences occurring at days 14 and 21 between treprostinil-treated BLM group and BLM/VEH group (Fig. 6e and f).

Treprostinil represses inflammatory signaling pathways

Nuclear factor-κB (NF-κB) is a transcription factor involved in the regulation of several proinflammatory pathways. Phosphorylation and subsequent degradation of the κB inhibitor (IκB) results in NF-κB activation. Mitogen-activated protein kinases (MAPKs) include the extracellular signal-regulated kinase (ERK), the c-Jun N-terminal kinases (JNK) and the p38 isoforms, which participate in cellular processes activated by various stimuli. Thus, we sought to study whether the aforementioned molecules are affected by pulmonary fibrosis induction and by treatment with treprostinil. The effect of BLM and TREP on ERK, p38 and JNK phosphorylation is presented in (Fig. 7a–f). BLM induced phosphorylation of IκBα inhibitory subunit leading to NF-κB activation (Fig. 7g and h). JNK and IκBα phosphorylation were inhibited by treprostinil (Fig. 7e and g) and these data were accordingly quantified to check statistical significance (Fig. 7f and h).

Discussion

As reported, in this study an experimental animal model of IPF was used to test the efficacy of a stable prostacyclin analogue when administrated through the inhaled route. Treprostinil is a prostanoid analogue that has been introduced as a specific treatment for pulmonary arterial hypertension following a randomized control trial that demonstrated its safety and efficacy.[23] Since then it has been a valuable asset, under different formulations, in the treatment of PAH patients.[24] To our knowledge, this is the first time that administration of treprostinil was proven to be beneficial in BLM-induced pulmonary inflammation, vascular remodeling, and fibrosis in mice. Our results indicate that orotracheal administration of treprostinil twice daily preserves lung function, reduces cellular accumulation, attenuates endothelial barrier disruption, attenuates vascular muscularization, preserves lung structure and diminishes collagen deposition in the lung. Moreover, treprostinil reduced MAPK and NF-κB activation, suggesting a role in lung inflammation. Daily treatment with this prostacyclin analogue through inhalation adequately mimicked human administration of inhaled treprostinil and provided a non-invasive way for the compound to the injured area, as opposed to invasive routes (e.g. intravenous or subcutaneous) that could cause discomfort and side-effects.[25,26]

Exposure to BLM causes acute excessive cell accumulation, edema formation and, in later stages, ECM deposition and distorted lung architecture. Treprostinil administration had beneficial effects in all the examined aforementioned features and at all time points, thus indicating multiple actions. Lung function was preserved at most time points, with lung mechanics of the prostacyclin analogue-treated group in early inflammatory phase (days 7, 14) approaching control values. Our results are supported by previous findings reporting the effects of inhaled PGI_2 on lowering airway resistance and improving lung compliance in a PH model.[27] Additionally, another PGI_2 analogue was recently shown to maintain lung function in BLM-challenged mice[28] and COX_2-derived prostacyclin managed to prevent BLM-induced pulmonary fibrosis using genetically modified mice.[10] Overall, accumulative data support that administration of prostanoids can be beneficial to lung function, a phenomenon also supported by our findings. Improvement of respiratory function is of great importance as it may improve life quality.[29]

Inflammatory cell accumulation was present in our BLM model, with the dominant cell types being macrophages, lymphocytes and neutrophils. Treprostinil managed to

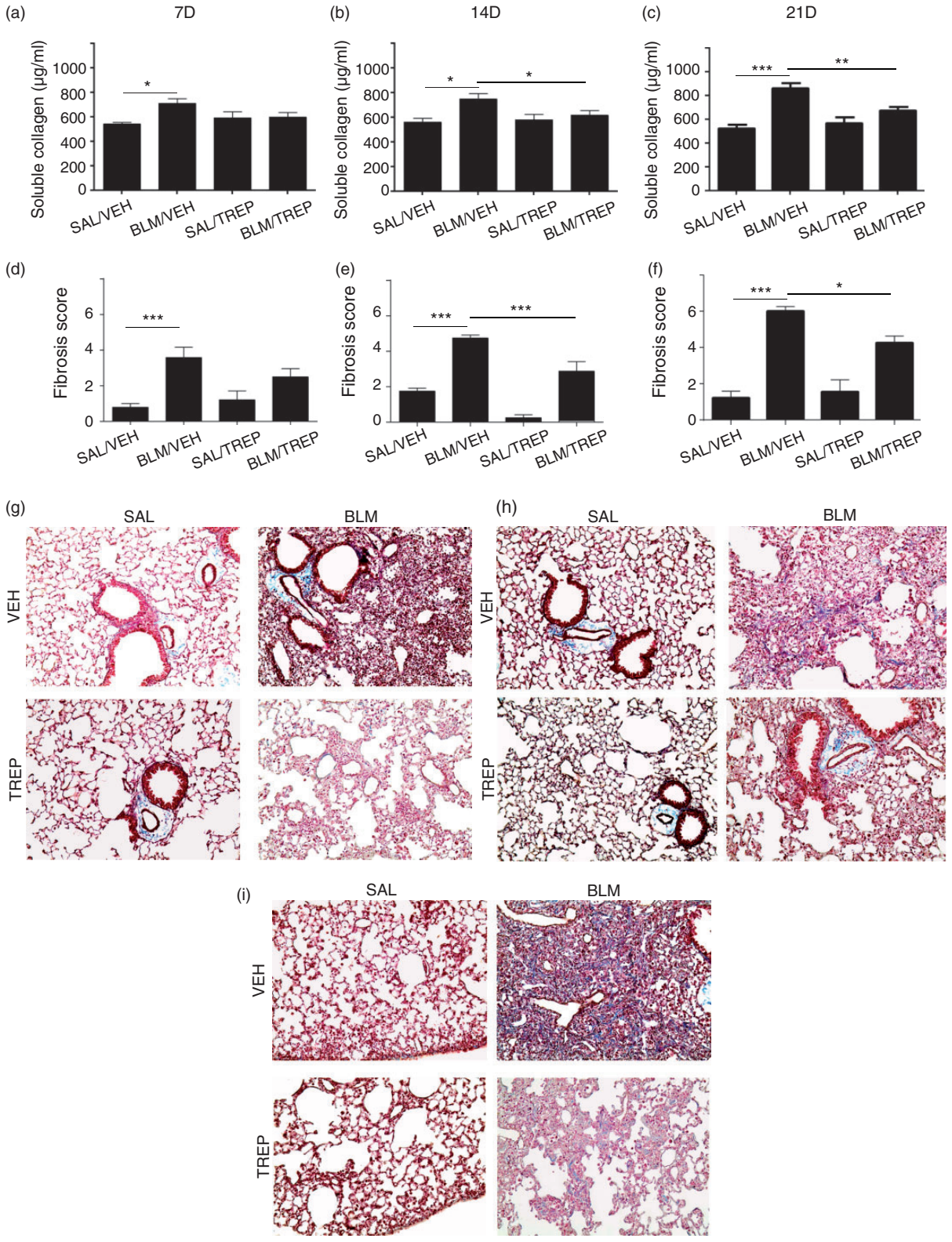

Fig. 5. Orotracheal administration of treprostinil (TREP) attenuates collagen deposition in bleomycin (BLM)-challenged mouse lungs. (a–c) Soluble collagen determination in lung extracts as measured by Sircol collagen kit 7, 14 and 21 days post BLM respectively. (g–i): Representative Masson staining of lung sections from samples collected at the aforementioned time points (g: 7D, h: 14D, i: 21D). Fibrotic injury in lung sections from all groups was given a score in order to be quantified and as shown in (d–f) the BLM/TREP group score was lower compared to BLM/VEH group. Results are expressed as mean ± SEM, $n = 9–10$ mice per group. One-way ANOVA followed by Newman–Keuls post hoc test was used for comparison among groups. SAL: saline; VEH: vehicle; 7D: 7 days; 14D: 14 days; 21D: 21 days.

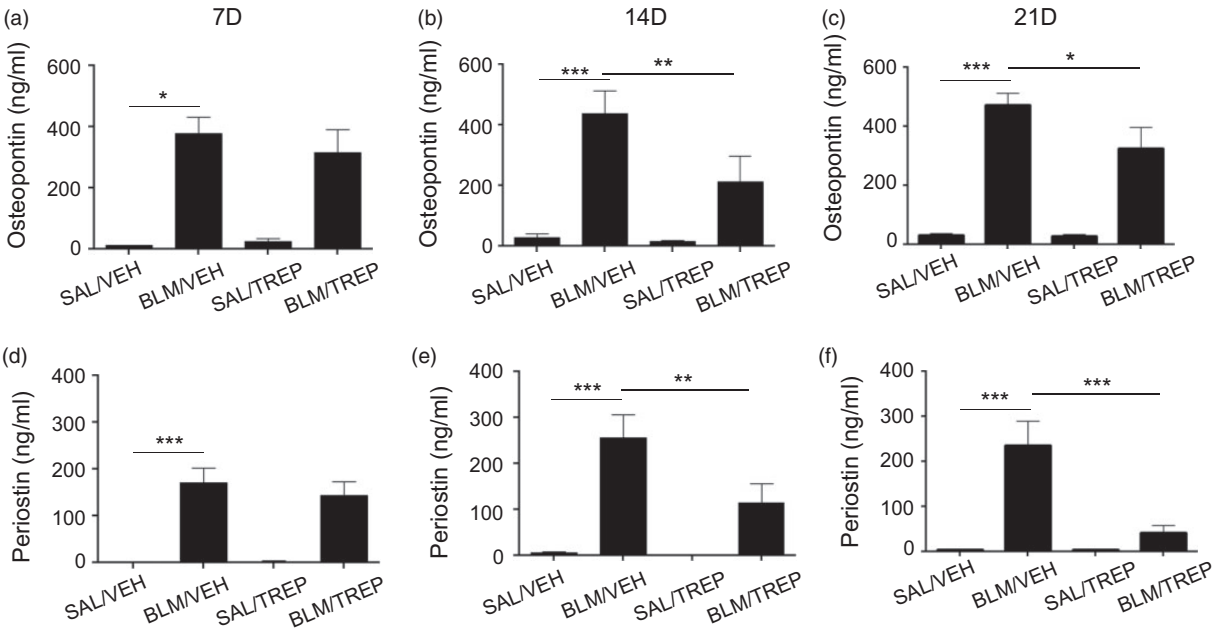

Fig. 6. Effect of treprostinil (TREP) on the production of osteopontin and periostin. Concentration of osteopontin (a–c) and periostin (d–f) was measured by ELISA in BALF collected 7, 14 and 21days post bleomycin (BLM). Results are expressed as mean ± SEM, $n = 9$–10 mice per group. One-way ANOVA followed by Newman–Keuls post hoc test was used for comparison among groups. SAL: saline; VEH: vehicle; 7D: 7 days; 14D: 14 days; 21D:21 days.

prevent BLM-induced pleocytosis at all time points and to attenuate increased total protein content in the alveolar space. It has been recently shown that increased peripheral monocytes are associated with poor outcome in patients with fibrotic diseases.[30] We cannot provide related information and this is a limitation of our study. To further examine the role of vascular endothelial barrier in the observed vascular leak, we tested the expression of VE-cadherin, a compound essential for the adequate endothelial barrier function. In accordance with the BLM-induced downregulation of VE-cadherin expression in human umbilical vein endothelial cells (HUVECs),[31] in our model, VE-cadherin was slightly, although significantly, reduced by BLM at one time point with no effect of treprostinil. Thus, the contribution of this molecule in the observed vascular leak, and presumably the endothelial barrier disruption involved, appears minimal.

Prostaglandins have been shown to possess anti-inflammatory actions in human and murine lungs, explained possibly by an imbalance between PGI_2 and TXA_2.[7,10,32] Increased levels of TXA_2 are also linked to neutrophil adhesion and pulmonary vascular permeability,[33] while BLM-induced BALF cellularity and protein content was previously attenuated by a prostacyclin agonist through controlling TXA_2 synthesis.[11] Over-expression of PGI_2 synthase attenuated inflammation in BLM-challenged mouse lungs without, though, reducing plasma protein leakage.[34] Overall, in vitro and in vivo studies have proven the barrier protective actions of prostacyclin analogues in different experimental models.[35–37]

BLM has already been shown to induce pulmonary vascular remodeling.[22] Accordingly, in our study, BLM increased vascular muscularization, a phenomenon attenuated by treprostinil. The latter implies that TREP might also attenuate the PH observed in patients with pulmonary fibrosis, since pulmonary vascular remodeling has a central role in the development of PH. In fact, the aforementioned positive results of TREP in this disease model, may suggest a potential therapeutic effect in PH under chronic lung diseases,[4] i.e. in Group 3 PH patients,[38] but this needs to be investigated.

Induction of inflammatory cells in IPF promotes the production of profibrotic agents, the differentiation of fibroblasts into myofibroblasts, and ultimately the large production of ECM components. In our model, BLM instillation led to a dramatic increase of soluble collagen in murine lungs with a significant deformation of normal lung structure and collagen deposition into lung parenchyma. These effects were all ameliorated by the stable prostacyclin analogue used in this study. In support of our results, prostanoids were previously implicated in fibrotic processes. Prostaglandin D_2 (PGD_2) was recently reported to protect mice from BLM-induced fibrosis,[39] while several other studies indicated PGE_2 as a dominant prostaglandin involved in fibrotic pathways.[40–42] TXA_2 also exerts fibrotic properties, and for an antifibrotic phenotype to be induced its expression must be suppressed.[33]

In support of our results, previous findings highlighted the possible clinical utility of prostacyclin analogues in IPF treatment. Prostacyclin analogs seemed to be beneficial

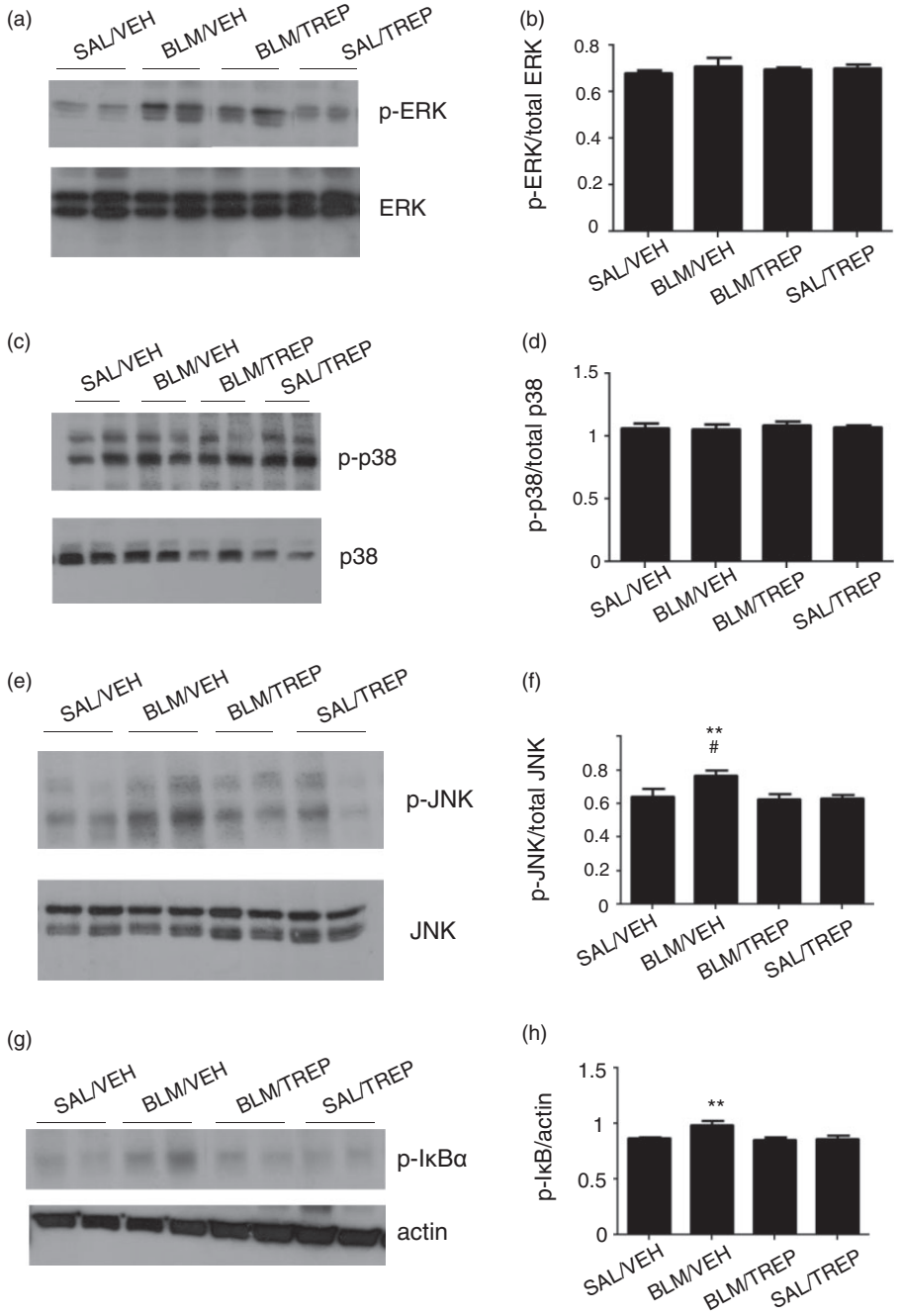

Fig. 7. Orotracheal administration of treprostinil (TREP) reduces phosphorylation of IκB and JNK. (a, c, e, g): Representative Western blots for p-ERK, p-p38, p-JNK and p-IκBα in mouse lung homogenates of samples collected 21 days post bleomycin (BLM)-challenge or vehicle (VEH). Total levels of MAPKs and actin were used as loading controls. (b, d, f, h): Quantification of protein levels after normalization is shown for each molecule. One-way ANOVA was used for comparison among groups and was followed by Tukey's multiple comparisons test. Data are expressed as means ± SEM. Differences between BLM/VEH and SAL/VEH groups are shown by $^{\#}$ ($^{\#}p < 0.05$); differences between BLM/VEH group and BLM/TREP group are shown by *. SAL: saline.

against fibrotic procedures, as they were shown to inhibit fibroblast migration,[9] to reduce production of connective tissue growth factor (CTGF) in fibroblasts from skin of systemic sclerosis (SSc)-suffering patients,[43] and to block TGF-β-induced fibrosis in rats.[44] Treprostinil in particular blocked the recruitment of bone marrow circulating fibrocytes in a chronic hypoxic PH model.[14] Finally and more recently an inhaled treprostinil prodrug was shown to attenuate collagen deposition in lungs of BLM-treated rats.[45]

As diagnosis and prognosis of IPF remain extremely challenging,[1] several molecules have been proposed as possible markers, underlying the need to monitor disease presence and/or progression. A potent biomarker of IPF is osteopontin (OPN),[46] a glycosylated phosphoprotein

exerting proinflammatory and profibrotic properties. OPN is highly upregulated in IPF lungs,[47] in BALF of IPF patients and in serum of interstitial lung disease (ILD) patients when compared with controls.[48] We observed increased levels of OPN in mouse BALF due to BLM exposure and our finding is consistent with previous studies on experimental lung fibrosis.[49] OPN is suggested to have a profibrotic effect in disease development[50] and to induce fibroblast growth and migration.[47] Treprostinil administration attenuated OPN increase in our experimental setting. This is further supported by another study showing that prostacyclin overexpression restores OPN levels in mouse osteoblasts.[51]

Periostin, a matricellular protein participating in wound healing and fibrosis[52,53] was the second molecule examined. Periostin is elevated in IPF lungs, with this increase mainly observed at fibroblast foci. Serum periostin levels are elevated in IPF patients and are correlated with disease progression.[53,54] In accordance with the above, we observed an increase of periostin in BALF of our BLM-challenged mice, a phenomenon attenuated by treprostinil administration. The former is supported by other studies demonstrating that in BLM-challenged lungs, deposition of periostin colocalized with fibrotic areas and that periostin genetic ablation reduced collagen deposition.[55] Moreover, periostin production by fibrocytes was proven instrumental in inducing myofibroblast differentiation.[56]

Focusing further on the molecular mechanisms underlying beneficial effects of treprostinil, apart from affecting osteopontin and periostin levels, we have also found affected inflammatory signalling pathways. More specifically, the BLM/TREP group showed reduced JNK and IκBα phosphorylation. This is in agreement with previous findings, supporting inhibition of NF-κB by treprostinil in human alveolar macrophages[57] and in murine dendritic cells.[58] Importantly, a study showing that intestinal inflammation is mediated by periostin through NF-κB activation[59] adds a link between molecules and functions investigated in our study. Another PGI_2 analogue was also able to suppress MAPK phosphorylation in human monocytes,[60] and inhibition of NF-κB activation in mouse lungs was previously shown to be effective in preventing BLM-induced pulmonary fibrosis.[61]

Other published results revealed that PGI_2 analogues could also protect from pulmonary dysfunction by preserving endothelial barrier integrity; these effects involved IκBα degradation, as well as MAP kinase activity.[31] Overall, it appears that in BLM-induced fibrosis studied here, apart from exerting anti-fibrotic effect, treprostinil also interferes with key inflammatory processes.

Conclusion

Our experiments show that daily administration of treprostinil via inhalation performed in the preventive treatment manner attenuated BLM-induced lung injury and fibrosis in mice. Respiratory function was preserved at a large degree, and less affected histopathological areas were observed. BLM-induced pulmonary vascular remodeling was attenuated by treprostinil, implying potential therapeutic efficacy in PH related to pulmonary fibrosis and other diseases related to Group 3 PH. Finally, inflammation and fibrosis were decreased, thus suggesting new insights in potential pharmacological treatments for severe and still incurable pulmonary fibrosis.

Authors' contributions

SEO, AK, DK and RTS conceived and designed the study. INik and NM acquired, analysed and interpreted data. XT and AP acquired data. CM, INin and VA analysed and interpreted data. All authors drafted and revised the manuscript, approved the final version and agreed to be accountable for all aspects of the work.

Conflict of interest

SEO has received research grants, and/or honoraria, and/or sponsoring to attend scientific meetings from United Therapeutics and Galenica–Ferrer. All other co-authors declare no conflicts of interest.

Funding

This study was funded (TRE-NC-004) and drug supply was provided by the United Therapeutics Corporation (Silver Spring, MD). It was additionally funded by a research grant from Galenica–Ferrer (1348/2015), both to SEO.

References

1. Tzouvelekis A, Tzilas V, Papiris S, et al. Diagnostic and prognostic challenges in Idiopathic pulmonary fibrosis: a patient's "Q and A" approach. *Pulm Pharmacol Ther* 2017; 42: 21–24.
2. Fujimoto H, Kobayashi T and Azuma A. Idiopathic pulmonary fibrosis: treatment and prognosis. *Clin Med Insights Circul Respir Pulm Med* 2015; 9: 179–185.
3. Betensley A, Sharif R and Karamichos D. A Systematic review of the role of dysfunctional wound healing in the pathogenesis and treatment of idiopathic pulmonary fibrosis. *J Clin Med* 2016; 6(1).
4. Nathan SD, Barbera JA, Gaine SP, et al. Pulmonary hypertension in chronic lung disease and hypoxia. *Eur Respir J* 2019; 53: 1801914.
5. Richeldi L, du Bois RM, Raghu G, et al. Efficacy and safety of nintedanib in idiopathic pulmonary fibrosis. *N Engl J Med* 2014; 370: 2071–2082.
6. Mouratis MA and Aidinis V. Modeling pulmonary fibrosis with bleomycin. *Curr Opin Pulm Med* 2011; 17: 355–361.
7. Soberman RJ and Christmas P. Revisiting prostacyclin: new directions in pulmonary fibrosis and inflammation. *Am J Physiol Lung Cell Mol Physiol* 2006; 291: L142–143.
8. Cruz-Gervis R, Stecenko AA, Dworski R, et al. Altered prostanoid production by fibroblasts cultured from the lungs of human subjects with idiopathic pulmonary fibrosis. *Respir Res* 2002; 3: 17.
9. Kohyama T, Liu X, Kim HJ, et al. Prostacyclin analogs inhibit fibroblast migration. *Am J Physiol Lung Cell Mol Physiol* 2002; 283: L428–432.

10. Lovgren AK, Jania LA, Hartney JM, et al. COX-2-derived prostacyclin protects against bleomycin-induced pulmonary fibrosis. *Am J Physiol Lung Cell Mol Physiol* 2006; 291: L144–156.
11. Murakami S, Nagaya N, Itoh T, et al. Prostacyclin agonist with thromboxane synthase inhibitory activity (ONO-1301) attenuates bleomycin-induced pulmonary fibrosis in mice. *Am J Physiol Lung Cell Mol Physiol* 2006; 290: L59–65.
12. Bozyk PD and Moore BB. Prostaglandin E2 and the pathogenesis of pulmonary fibrosis. *Am J Respir Cell Mol Biol* 2011; 45: 445–452.
13. Choung J, Taylor L, Thomas K, et al. Role of EP2 receptors and cAMP in prostaglandin E2 regulated expression of type I collagen alpha1, lysyl oxidase, and cyclooxygenase-1 genes in human embryo lung fibroblasts. *J Cell Biochem* 1998; 71: 254–263.
14. Nikam VS, Schermuly RT, Dumitrascu R, et al. Treprostinil inhibits the recruitment of bone marrow-derived circulating fibrocytes in chronic hypoxic pulmonary hypertension. *Eur Respir J* 2010; 36: 1302–1314.
15. Manitsopoulos N, Kotanidou A, Magkou C, et al. Treprostinil administration attenuates bleomycin-induced lung fibrosis in mice. [abstract]. *Eur Resp J* 2015; 46: PA3837.
16. Yang J, Li X, Al-Lamki RS, et al. Smad-dependent and smad-independent induction of id1 by prostacyclin analogues inhibits proliferation of pulmonary artery smooth muscle cells in vitro and in vivo. *Circul Res* 2010; 107: 252–262.
17. Manitsopoulos N, Nikitopoulou I, Maniatis NA, et al. Highly selective endothelin-1 receptor A inhibition prevents bleomycin-induced pulmonary inflammation and fibrosis in mice. *Respiration* 2018; 95: 122–136.
18. Manali ED, Moschos C, Triantafillidou C, et al. Static and dynamic mechanics of the murine lung after intratracheal bleomycin. *BMC Pulm Med* 2011; 11: 33.
19. Murao Y, Loomis W, Wolf P, et al. Effect of dose of hypertonic saline on its potential to prevent lung tissue damage in a mouse model of hemorrhagic shock. *Shock* 2003; 20: 29–34.
20. Dahal BK, Kosanovic D, Pamarthi PK, et al. Therapeutic efficacy of azaindole-1 in experimental pulmonary hypertension. *Eur Respir J* 2010; 36: 808–818.
21. Hubner RH, Gitter W, El Mokhtari NE, et al. Standardized quantification of pulmonary fibrosis in histological samples. *Biotechniques* 2008; 44: 507–511, 514–517.
22. Cortijo J, Iranzo A, Milara X, et al. Roflumilast, a phosphodiesterase 4 inhibitor, alleviates bleomycin-induced lung injury. *Br J Pharmacol* 2009; 156: 534–544.
23. Simonneau G, Barst RJ, Galie N, et al. Continuous subcutaneous infusion of treprostinil, a prostacyclin analogue, in patients with pulmonary arterial hypertension: a double-blind, randomized, placebo-controlled trial. *Am J Respir Crit Care Med* 2002; 165: 800–804.
24. Galie N, Humbert M, Vachiery JL, et al. 2015 ESC/ERS Guidelines for the diagnosis and treatment of pulmonary hypertension: the joint task force for the diagnosis and treatment of pulmonary hypertension of the European Society of Cardiology (ESC) and the European Respiratory Society (ERS): endorsed by: association for European Paediatric and Congenital Cardiology (AEPC), International Society for Heart and Lung Transplantation (ISHLT). *Eur Heart J* 2016; 37: 67–119.
25. Mirza S and Foley RJ. Clinical utility of treprostinil and its overall place in the treatment of pulmonary arterial hypertension. *Clin Med Insights Circul Respir Pulm Med* 2012; 6: 41–50.
26. Buckley MS, Berry AJ, Kazem NH, et al. Clinical utility of treprostinil in the treatment of pulmonary arterial hypertension: an evidence-based review. *Core Evid* 2014; 9: 71–80.
27. Dani C, Pavoni V, Corsini I, et al. Inhaled nitric oxide combined with prostacyclin and adrenomedullin in acute respiratory failure with pulmonary hypertension in piglets. *Pediatric Pulmonol* 2007; 42: 1048–1056.
28. Zhu Y, Liu Y, Zhou W, et al. A prostacyclin analogue, iloprost, protects from bleomycin-induced pulmonary fibrosis in mice. *Respir Res* 2010; 11: 34.
29. Flaherty KR, Andrei AC, Murray S, et al. Idiopathic pulmonary fibrosis: prognostic value of changes in physiology and six-minute-walk test. *Am J Resp Crit Care Med* 2006; 174: 803–809.
30. Scott MKD, Quinn K, Li Q, et al. Increased monocyte count as a cellular biomarker for poor outcomes in fibrotic diseases: a retrospective, multicentre cohort study. *Lancet Respir Med* 2019; 7: 497–508.
31. Zhang W, Chen G, Ren JG and Zhao YF. Bleomycin induces endothelial mesenchymal transition through activation of mTOR pathway: a possible mechanism contributing to the sclerotherapy of venous malformations. *Br J Pharmacol* 2013; 170: 1210–1220.
32. Chandler DB, Giri SN, Chen Z, et al. The in vitro synthesis and degradation of prostaglandins during the development of bleomycin-induced pulmonary fibrosis in hamsters. *Prostagland Leukotrienes Med* 1983; 11: 11–31.
33. Schulman CI, Wright JK, Nwariaku F, et al. The effect of tumor necrosis factor-alpha on microvascular permeability in an isolated, perfused lung. *Shock* 2002; 18: 75–81.
34. Zhou W, Dowell DR, Geraci MW, et al. PGI synthase overexpression protects against bleomycin-induced mortality and is associated with increased Nqo 1 expression. *Am J Physiol Lung Cell Mol Physiol* 2011; 301: L615–622.
35. Birukova AA, Wu T, Tian Y, et al. Iloprost improves endothelial barrier function in lipopolysaccharide-induced lung injury. *Eur Respir J* 2013; 41: 165–176.
36. Birukova AA, Zagranichnaya T, Fu P, et al. Prostaglandins PGE(2) and PGI(2) promote endothelial barrier enhancement via PKA- and Epac1/Rap1-dependent Rac activation. *Exp Cell Res* 2007; 313: 2504–2520.
37. Fukuhara S, Sakurai A, Sano H, et al. Cyclic AMP potentiates vascular endothelial cadherin-mediated cell-cell contact to enhance endothelial barrier function through an Epac-Rap1 signaling pathway. *Mol Cell Biol* 2005; 25: 136–146.
38. Simonneau G, Montani D, Celermajer DS, et al. Haemodynamic definitions and updated clinical classification of pulmonary hypertension. *Eur Respir J* 2019; 53: 1801913.
39. Kida T, Ayabe S, Omori K, et al. Prostaglandin D2 attenuates bleomycin-induced lung inflammation and pulmonary fibrosis. *PLoS One* 2016; 11: e0167729.
40. Dackor RT, Cheng J, Voltz JW, et al. Prostaglandin E(2) protects murine lungs from bleomycin-induced pulmonary fibrosis and lung dysfunction. *Am J Physiol Lung Cell Mol Physiol* 2011; 301: L645–655.
41. Vancheri C, Sortino MA, Tomaselli V, et al. Different expression of TNF-alpha receptors and prostaglandin E(2) Production in normal and fibrotic lung fibroblasts: potential

implications for the evolution of the inflammatory process. *Am J Respir Cell Mol Biol* 2000; 22: 628–634.
42. Wilborn J, Crofford LJ, Burdick MD, et al. Cultured lung fibroblasts isolated from patients with idiopathic pulmonary fibrosis have a diminished capacity to synthesize prostaglandin E2 and to express cyclooxygenase-2. *J Clin Invest* 1995; 95: 1861–1868.
43. Stratton R, Shiwen X, Martini G, et al. Iloprost suppresses connective tissue growth factor production in fibroblasts and in the skin of scleroderma patients. *J Clin Invest* 2001; 108: 241–250.
44. Stratton R, Rajkumar V, Ponticos M, et al. Prostacyclin derivatives prevent the fibrotic response to TGF-beta by inhibiting the Ras/MEK/ERK pathway. *FASEB J* 2002; 16: 1949–1951.
45. Corboz MR, Zhang J, LaSala D, et al. Therapeutic administration of inhaled INS1009, a treprostinil prodrug formulation, inhibits bleomycin-induced pulmonary fibrosis in rats. *Pulm Pharmacol Ther* 2018; 49: 95–103.
46. Ley B, Brown KK and Collard HR. Molecular biomarkers in idiopathic pulmonary fibrosis. *Am J Physiol Lung Cell Mol Physiol* 2014; 307: L681–691.
47. Pardo A, Gibson K, Cisneros J, et al. Up-regulation and profibrotic role of osteopontin in human idiopathic pulmonary fibrosis. *PLoS Med* 2005; 2: e251.
48. Kadota J, Mizunoe S, Mito K, et al. High plasma concentrations of osteopontin in patients with interstitial pneumonia. *Respir Med* 2005; 99: 111–117.
49. Kaminski N, Allard JD, Pittet JF, et al. Global analysis of gene expression in pulmonary fibrosis reveals distinct programs regulating lung inflammation and fibrosis. *Proc Natl Acad Sci U S A* 2000; 97: 1778–1783.
50. Takahashi F, Takahashi K, Okazaki T, et al. Role of osteopontin in the pathogenesis of bleomycin-induced pulmonary fibrosis. *Am J Respir Cell Mol Biol* 2001; 24: 264–271.
51. Chabbi-Achengli Y, Launay JM, Maroteaux L, et al. Serotonin 2B receptor (5-HT2B R) signals through prostacyclin and PPAR-ss/delta in osteoblasts. *PLoS One* 2013; 8: e75783.
52. Kudo A. Periostin in fibrillogenesis for tissue regeneration: periostin actions inside and outside the cell. *Cell Mol Life Sci* 2011; 68: 3201–3207.
53. Naik PK, Bozyk PD, Bentley JK, et al. Periostin promotes fibrosis and predicts progression in patients with idiopathic pulmonary fibrosis. *Am J Physiol Lung Cel Mol Physiol* 2012; 303: L1046–1056.
54. Okamoto M, Hoshino T, Kitasato Y, et al. Periostin, a matrix protein, is a novel biomarker for idiopathic interstitial pneumonias. *Eur Respir J* 2011; 37: 1119–1127.
55. Uchida M, Shiraishi H, Ohta S, et al. Periostin, a matricellular protein, plays a role in the induction of chemokines in pulmonary fibrosis. *Am J Respir Cell Mol Biol* 2012; 46: 677–686.
56. Ashley SL, Wilke CA, Kim KK, et al. Periostin regulates fibrocyte function to promote myofibroblast differentiation and lung fibrosis. *Mucosal Immunol* 2017; 10: 341–351.
57. Raychaudhuri B, Malur A, Bonfield TL, et al. The prostacyclin analogue treprostinil blocks NFkappaB nuclear translocation in human alveolar macrophages. *J Biol Chem* 2002; 277: 33344–33348.
58. Zhou W, Hashimoto K, Goleniewska K, et al. Prostaglandin I2 analogs inhibit proinflammatory cytokine production and T cell stimulatory function of dendritic cells. *J Immunol* 2007; 178: 702–710.
59. Koh SJ, Choi Y, Kim BG, et al. Matricellular protein periostin mediates intestinal inflammation through the activation of nuclear factor kappaB signaling. *PLoS One* 2016; 11: e0149652.
60. Wang WL, Kuo CH, Chu YT, et al. Prostaglandin I(2) analogues suppress TNF-alpha expression in human monocytes via mitogen-activated protein kinase pathway. *Inflamm Res* 2011; 60: 655–663.
61. Inayama M, Nishioka Y, Azuma M, et al. A novel IkappaB kinase-beta inhibitor ameliorates bleomycin-induced pulmonary fibrosis in mice. *Am J Respir Crit Care Med* 2006; 173: 1016–1022.